Pole-Zero, Zero-Pole Canceling Input Shapers

Tarunraj Singh
Professor
Fellow ASME Department of Mechanical and Aerospace Engineering,
SUNY at Buffalo,
Buffalo, NY 14260

This paper presents the development of an input-shaper/time-delay filter, which exploits knowledge of the zeros of a minimum-phase transfer function to reduce the output-transition time for a rest-to-rest maneuver problem, compared to the traditional zero vibration (ZV) input shaper. The maneuver time of the robust input shaper presented in this work will correspondingly have a smaller maneuver time compared to the zero vibration derivative (ZVD) input-shaper. The shaped profile is changing with time even after the completion of the maneuver similar to postactuation controllers. All the traditional technique for addressing multiple modes and desensitizing the filter over a specified domain of uncertainties are applicable to the technique presented in this paper. [DOI: 10.1115/1.4004576]

Keywords: input shaper, postactuation, vibration control

1 Introduction

The growth in the interest of input shapers/time-delay filters [1–4] for application, which are characterized by self-excited vibratory motion has been growing over the past decade. Western Digital's *Whisper Drive* reduces acoustic excitation using a *digital dynamic seek shaping* [5], which is essentially the implementation of a method to shape the current input to the arm actuator to minimize noise. Jerk limiting techniques to achieve the same objective have also been proposed by Hindle and Singh [6] and Singh[7]. Crane manufacturers are now integrating input shapers into their drive pendants [8]. Input shaping has been used for precise control of wafer scanners and has recently been applied to atomic force microscopy (AFM) ([9]) on coordinate measuring machines [10–12] and on Micro-Electro-Mechanical System (MEMS) MEMS devices[1]. The simplicity of the input shaper in conjunction with the ability to include it in legacy systems without the requirement of additional sensors/actuators makes its adoption easy to accept.

One of the shortcomings of the early input-shapers (posicast control [13]) was their sensitivity to modeling uncertainties. Singer and Seering [2] presented a simple technique, which forces the displacement and velocity states and their sensitivities to errors in system frequency or damping ratio to zero, when subject to a series of impulses. They referred to their technique as *input shaping*. Singh and Vadali [3] subsequently illustrated that using the zeros of the transfer function of a time-delay filter to cancel the underdamped poles of the system resulted in a solution, which was identical to the input-shaper. Over the past decade, techniques which desensitize the residual energy in the proximity of the nominal model and the design of minimax filters, which design robust filters over a prescribed domain of uncertainties have been developed and adopted for various applications [14,15]. The consequence of increasing the robustness to modeling errors is an increase in the maneuver time. In many applications this tradeoff is palatable. However, if one desires to improve the performance of the robust input shapers, one needs to develop techniques which exploit knowledge of the zeros of the transfer function, which to-date have been ignored by the input-shaping/time-delay filtering community. Perez and Devasia [16] present a detailed development of output point-to-point transition and compare the solution to the state-to-state transition problem where the input energy is to be minimized. They decouple the states into stable, unstable, and marginally stable states. They then exploit the dynamics of the stable and unstable states to generate pre-actuation and postactuation control, which do not perturb the system output. They illustrate that the pre-actuation and postactuation can result in reduced consumption of input energy. Iamratanakul et al. [17] illustrate the pre-actuation and postactuation control strategy on a dual stage actuator for a disk drive and demonstrate a 65% reduction in the consumed energy compared to state-to-state transition controllers.

This works present a simple technique to improve the performance of traditional input-shapers/time-delay filters for a class of stable or marginally stable linear systems. Systems whose input–output transfer functions include left-half plane zeros can benefit from the technique presented in this paper. First, the design of time-delay prefilters or input shapers, which cancel the zeros of the plants are presented for systems with one zero. Next, the approach is extended to systems with second order zeros. Closed form expressions are derived for first and second order zeros, and the pole-zero canceling input shapers are illustrated on a simple example. Since, any numerator polynomial of a transfer function can be factored into first and second order zeros, the proposed technique is generalized based on the developed pole-zero canceling prefilter. Finally, the proposed technique and a version, which accounts for uncertainties in model parameters, are illustrated on the pitch control of an aircraft.

2 Second Order System/Single Zero

2.1 Parameterization 1. The input-shaper/time-delay filter for a system with a transfer function

$$\frac{Y(s)}{U(s)} = G_p(s) = \frac{s+\alpha}{s^2+2\zeta\omega s+\omega^2}, \quad \alpha > 0 \tag{1}$$

is given by the transfer function

$$G(s) = \frac{A}{A+1} + \frac{1}{A+1}\exp(-sT) \tag{2}$$

where

$$T = \frac{\pi}{\omega\sqrt{1-\zeta^2}}, \quad A = \exp\left(\frac{\zeta\pi}{\sqrt{1-\zeta^2}}\right) \tag{3}$$

The input-shaper/time-delay filter includes a pair of zeros, which cancels the underdamped poles of the system located at $s = -\zeta\omega \pm j\omega\sqrt{1-\zeta^2}$. Since, the dc gain of the transfer function is $\frac{\alpha}{\omega^2}$, the transfer function of the input-shaper/time-delay filter $G(s)$ should be scaled by ω^2/α to ensure that the final value of the controlled system is the same as the reference input.

Contributed by the Dynamic Systems Division of ASME for publication in the JOURNAL OF DYNAMIC SYSTEMS, MEASUREMENT AND CONTROL. Manuscript received August 13, 2010; final manuscript received April 1, 2011; published online December 5, 2011. Assoc. Editor: Xubin Song.

[1] http://www.PolytecPI.com

Consider a parameterization of a time-delay filter, which cancels the poles and zeros of the plant, while satisfying the requirement that the output reach its desired position in minimum time. The parameterization of the time-delay filter is

$$G(s) = A + \frac{\exp(-sT)}{s+\alpha} \tag{4}$$

where a first order pole is included in the delayed term, which permits canceling the zero of the plant located at $s=-\alpha$. This filter will be referred to as a postactuation input shaper since the output of the prefilter continues to transition to its final value after time T. The goal of canceling the poles of the plant can be solved by determining the parameters A and T so that a pair of zeros of the time-delay filter cancel the underdamped poles of the system. The time-delay filter has zeros at $s=-\zeta\omega \pm j\omega\sqrt{1-\zeta^2}$, if:

$$G\left(s=-\zeta\omega \pm j\omega\sqrt{1-\zeta^2}\right) = 0 = A(s+\alpha) + \exp(-sT) \tag{5}$$

$$0 = A\left(-\zeta\omega \pm j\omega\sqrt{1-\zeta^2}+\alpha\right) + \exp\left(\left(\zeta\omega \mp j\omega\sqrt{1-\zeta^2}\right)T\right) \tag{6}$$

which can be rewritten by equating the real and imaginary parts to zero as

$$\exp(\zeta\omega T)\cos\left(\omega\sqrt{1-\zeta^2}T\right) = -A(-\zeta\omega+\alpha) \tag{7}$$

$$\exp(\zeta\omega T)\sin\left(\omega\sqrt{1-\zeta^2}T\right) = A\omega\sqrt{1-\zeta^2} \tag{8}$$

The ratio of Eqs. (8) and (7) leads to

$$\tan\left(\omega\sqrt{1-\zeta^2}T\right) = \frac{\omega\sqrt{1-\zeta^2}}{\zeta\omega-\alpha} \tag{9}$$

which can be used to solve for T

$$T = \pm\frac{n\pi}{\omega\sqrt{1-\zeta^2}} + \frac{1}{\omega\sqrt{1-\zeta^2}}\arctan\left(\frac{\omega\sqrt{1-\zeta^2}}{\zeta\omega-\alpha}\right) \tag{10}$$

where n is an integer. Sum of the square of Eqs. (7) and (8) leads to

$$\exp(2\zeta\omega T) = A^2\left(\alpha^2 - 2\zeta\omega\alpha + \omega^2\right) \tag{11}$$

which can be used to solve for A. To ensure that the final value of the output of the time-delay filter is the same as the reference input, the gains of the time-delay filter have to be scaled. The final value of the system subject to a unit step input is

$$K = \lim_{s\to 0}\frac{1}{s}sG(s)G_p(s) = \left(A+\frac{1}{\alpha}\right)\frac{\alpha}{\omega^2} \tag{12}$$

The final time delay filter is

$$G(s) = \frac{A}{K} + \frac{\exp(-sT)}{K(s+\alpha)} \tag{13}$$

Figure 1 illustrates the variation of the switch time, which is also the maneuver time as a function of the reciprocal of the location of the zero for a system with a natural frequency of 1 and a damping ratio of 0. This results in a graph where the origin corresponds to a zero located at $-\infty$, which corresponds to a system without a finite zero and the resulting solution should correspond to the standard input shaper solution (dashed line). Figure 1 illustrates the pole-zero canceling input shaper (postactuation filter) switch time is the same as that of the input shaper for $1/\alpha=0$. Likewise Fig. 2 illustrates that for $1/\alpha=0$, the gains of the filter coincide

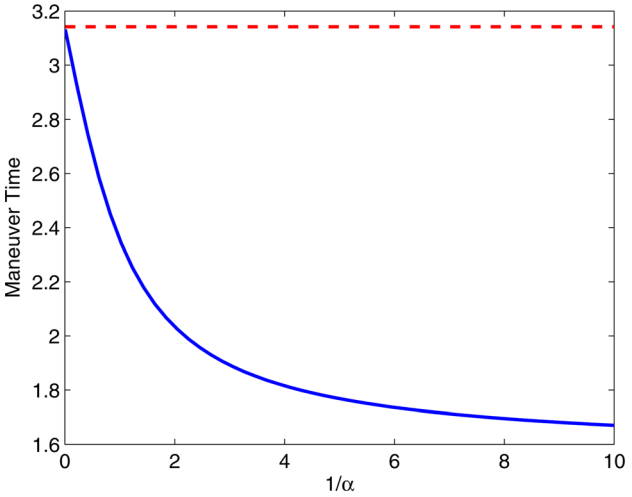

Fig. 1 Variation of switch time versus $\frac{1}{\alpha}$

with those of the standard input shapers. The solid line in Fig. 2 corresponds to A and decreases as the plant zero moves toward the origin. This implies that a smaller step input is initially applied to the system. The dashed line is the coefficient of the delay term of the postactuation input shaper. Figure 1 illustrates that as the zero location moves closer to the origin, the maneuver time decreases considerably compared to the standard input shaper.

2.1.1 Example. To illustrate the proposed technique, consider the example,

$$G_p(s) = \frac{s+1}{s^2+2} \tag{14}$$

We note that the dc gain is 0.5, which requires the final value of the output be scaled by 2 to track a desired reference input. The resulting solution is

$$G(s) = 0.7321 + 1.2679\frac{\exp(-1.5459s)}{s+1} \tag{15}$$

while the solution of the traditional input shaper/time-delay filter is

$$G(s) = 1.0 + 1.0\exp(-2.22144s) \tag{16}$$

which is a 30% reduction in the maneuver time. Figures 3(*a*) and 3(*b*) illustrate the evolution of the states and the corresponding reference profile. The solid line corresponds to the postactuation

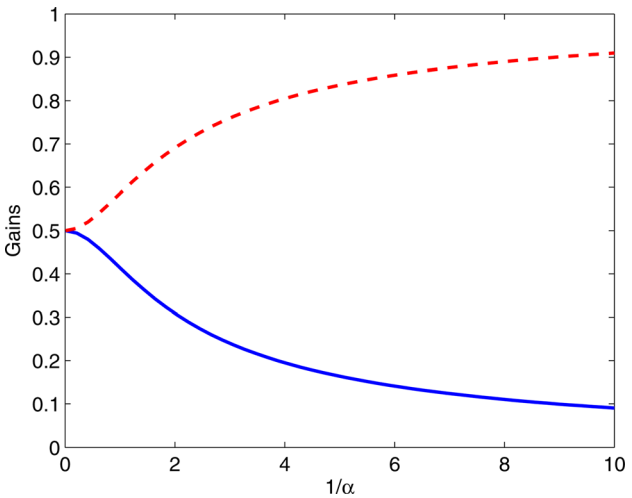

Fig. 2 Variation of gains versus $\frac{1}{\alpha}$

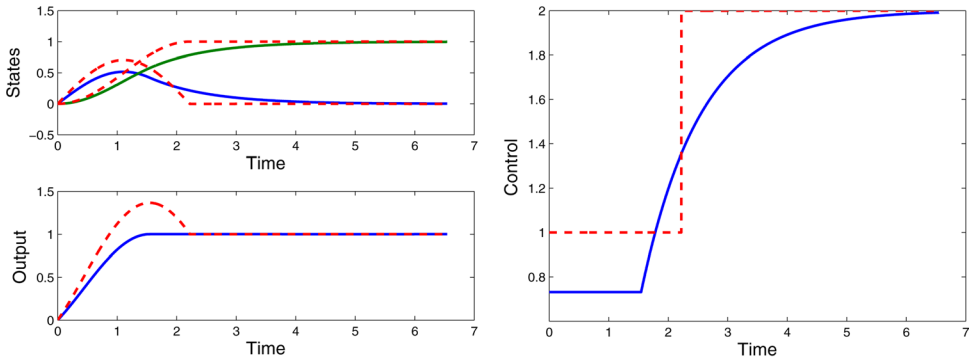

(a) Evolution of states (b) Control Profile

Fig. 3 Postactuated time-delay filter: (*a*) evolution of states; (*b*) control profile

filter, while the dashed line corresponds to the traditional input shaper. It can be seen that the output has reached the final value in 1.5459 s, while the states of the system are continuing to transition to their steady state values.

2.2 Parameterization 2. The parameterization of the postactuation filter in Sec. 2.1 associated a first order pole with the delayed input. A second parameterization where the first order pole is associated with the nondelayed term is proposed in this section

$$G(s) = \frac{A}{s+\alpha} + \exp(-sT) \tag{17}$$

The time-delay filter has zeros at $s = -\zeta\omega \pm j\omega\sqrt{1-\zeta^2}$, if

$$G(s = -\zeta\omega \pm j\omega\sqrt{1-\zeta^2}) = 0 = A + (s+\alpha)\exp(-sT) \tag{18}$$

$$0 = A + (-\zeta\omega \pm j\omega\sqrt{1-\zeta^2} + \alpha)\exp((\zeta\omega \mp j\omega\sqrt{1-\zeta^2})T) \tag{19}$$

which can be separated into two equations by equating the real and imaginary parts to zero, resulting in

$$A + \exp(\zeta\omega T)\left((-\zeta\omega+\alpha)\cos\left(\omega\sqrt{1-\zeta^2}T\right) + \omega\sqrt{1-\zeta^2}\sin\left(\omega\sqrt{1-\zeta^2}T\right)\right) = 0 \tag{20}$$

$$\exp(\zeta\omega T)\left(-(-\zeta\omega+\alpha)\sin\left(\omega\sqrt{1-\zeta^2}T\right) + \omega\sqrt{1-\zeta^2}\cos\left(\omega\sqrt{1-\zeta^2}T\right)\right) = 0 \tag{21}$$

Equations (20) and (21) can be used to solve for the switch time

$$\tan\left(\omega\sqrt{1-\zeta^2}T\right) = \frac{\omega\sqrt{1-\zeta^2}}{-\zeta\omega+\alpha} \tag{22}$$

which reduces to

$$T = \pm\frac{n\pi}{\omega\sqrt{1-\zeta^2}} + \frac{1}{\omega\sqrt{1-\zeta^2}}\text{arc tan}\left(\frac{\omega\sqrt{1-\zeta^2}}{-\zeta\omega+\alpha}\right) \tag{23}$$

where n is an integer. Equations (20) and (21) can also be used to solve for A

$$A = -\exp(\zeta\omega T)(\omega^2 - 2\zeta\omega\alpha + \alpha^2) \tag{24}$$

It can be seen that A is not influenced by the maneuver time for undamped systems ($\zeta = 0$). To ensure that the final value of the output of the system is the same as the reference input, the gains of the postactuation filter have to be scaled by the gain

$$K = (A+\alpha) \tag{25}$$

The postactuation prefilter is given by the transfer function

$$G_c(s) = \frac{A}{(A+\alpha)(s+\alpha)} + \frac{\exp(-sT)}{(A+\alpha)} \tag{26}$$

Figure 4 illustrates the variation of the switch time as a function of the location of the zero α. When $1/\alpha = 0$, which corresponds to a zero at $-\infty$, the postactuation filter should be coincident with the traditional input shaper. Figure 5 illustrates that the gain of the nondelayed term of the postactuation filter is consistently greater than 1, which is caused by the initial input transitioning to its final value as opposed to the standard input shaper, where a step input is applied at time zero.

Comparing Figs. 2 and 5, it is clear that by associating the first order pole with the final term of the postactuation filter generates prefilter gains that lie between zero and one, which are desirable to preclude large input by the actuators to track the reference inputs. The zeros of the transfer function of the system under

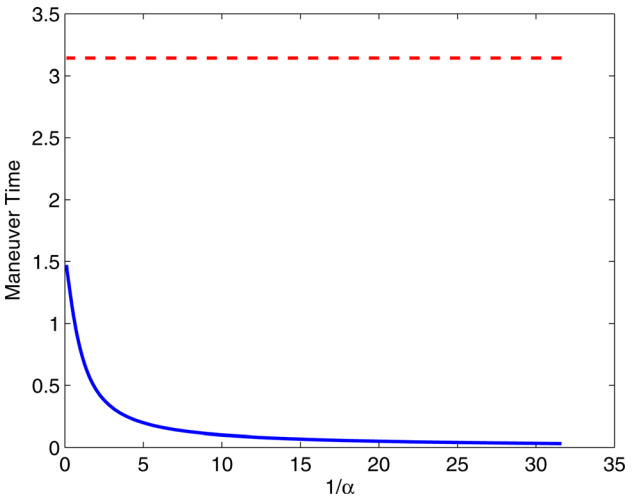

Fig. 4 Variation of switch time versus $\frac{1}{\alpha}$

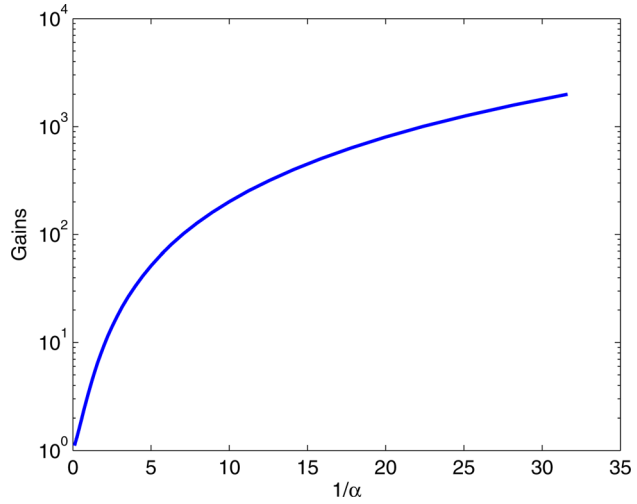

Fig. 5 Variation of gains versus $\frac{1}{\alpha}$

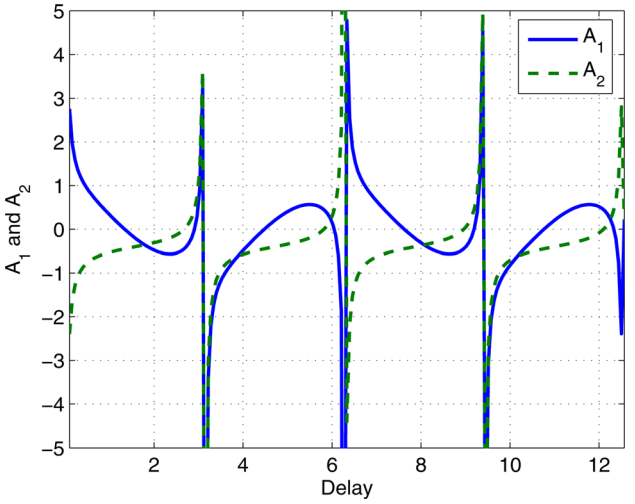

Fig. 6 Variation of gains versus *T*

consideration can be canceled by associating the poles with any delayed term of the postactuation filter. We will, however, only associate the pole with the largest delayed term since it results in solutions, which are reasonable to implement.

2.3 Parameterization 3. For discrete-time systems, the postactuation filter can be designed by parameterizing the time-delay filter as

$$G(s) = A_1 + A_2 \exp(-sT) + \frac{1}{s+\alpha}\exp(-sT) \tag{27}$$

where T is selected to be an integer multiple of the sampling time. The time-delay filter has zeros at $s = -\zeta\omega \pm j\omega\sqrt{1-\zeta^2}$, if

$$G\left(s = -\zeta\omega \pm j\omega\sqrt{1-\zeta^2}\right) = 0$$
$$= (A_1 + A_2\exp(-sT)) + \frac{\exp(-sT)}{(s+\alpha)} \tag{28}$$

which can be separated into two equations by equating the real and imaginary parts to zero, resulting in

$$\begin{bmatrix} 1 & e^{\zeta\omega T}\cos(\omega\sqrt{1-\zeta^2}T) \\ 0 & e^{\zeta\omega T}\sin(\omega\sqrt{1-\zeta^2}T) \end{bmatrix} \begin{Bmatrix} A_1 \\ A_2 \end{Bmatrix}$$
$$= \frac{e^{\zeta\omega T}}{\omega^2 - 2\zeta\omega\alpha + \alpha^2} \begin{bmatrix} (\alpha-\zeta\omega)\cos\left(\omega\sqrt{1-\zeta^2}T\right) - \omega\sqrt{1-\zeta^2}\sin\left(\omega\sqrt{1-\zeta^2}T\right) \\ -(\alpha-\zeta\omega)\sin\left(\omega\sqrt{1-\zeta^2}T\right) - \omega\sqrt{1-\zeta^2}\cos\left(\omega\sqrt{1-\zeta^2}T\right) \end{bmatrix} \tag{29}$$

For a specified T, the parameters A_1 and A_2 can be solved for easily.

Figure 6 illustrates the variation of the gains A_1 and A_2 as a function of the delay time T. One can see that the solution is singular when the damped natural frequency $\omega\sqrt{1-\zeta^2}$ is equal to multiple of π/T.

Since the steady state gain of the postactuation filter for a unit step input is

$$K = A_1 + A_2 + \frac{1}{\alpha} \tag{30}$$

The gains of the postactuation filter have to be normalized by K to ensure that the final value of the output of the postactuation filter is the same as the input. The normalized gains are plotted in Fig. 7. One can note that when $A_1 + A_2 = -1/\alpha$, the normalizing term K equals zero, which forces the gain to infinity. This is the reason why the gains in Fig. 7 become large for values of T other than when $\omega\sqrt{1-\zeta^2}T$ is equal to multiples of π. Specifically, this occurs for $T = 1.4716$, 4.4168, 7.7548, and 10.70 in Fig. 7.

Since the use of a postactuation filter which includes large changes in the reference profile can excite unmodeled dynamics, it is desirable to design a postactuation filter, which results in a monotonic increase in the reference input toward the steady state value. This results in a benign demand on the actuator and a graceful transition to the final states. Figure 8 illustrates the region over the space of permissible delay time T where the gains are positive.

3 Second Order System/Two Zeros

To design a pole-zero canceling input shaper (postactuation time-delay filter) for a system with a transfer function

$$G_p(s) = \frac{s^2 + 2\phi\psi s + \psi^2}{s^2 + 2\zeta\omega s + \omega^2}, \quad 0 \le \phi \le 1, \psi > 0 \tag{31}$$

We require a time-delay filter with a transfer function

$$G(s) = A + \frac{\exp(-sT)}{s^2 + 2\phi\psi s + \psi^2} \tag{32}$$

which cancels the zeros of the system given by the equation

$$s^2 + 2\phi\psi s + \psi^2 = 0 \tag{33}$$

To cancel the underdamped poles of the system located at $s = -\zeta\omega \pm j\omega\sqrt{1-\zeta^2}$, we substitute $s = -\zeta\omega \pm j\omega\sqrt{1-\zeta^2}$ into Eq. (32) and equating the real and imaginary parts to zero, we have

$$\exp(\zeta\omega T)\cos\left(\omega\sqrt{1-\zeta^2}T\right) = A\left(-2\zeta^2\omega^2 + \omega^2 + 2\phi\psi\zeta\omega - \psi^2\right) \tag{34}$$

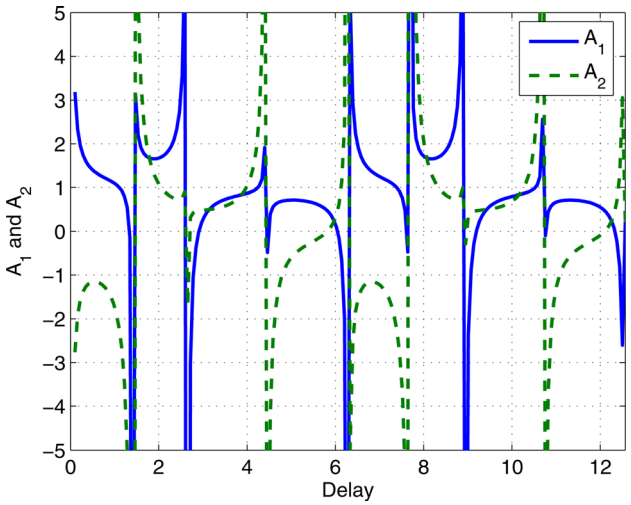

Fig. 7 Variation of normalized gains versus *T*

$$\exp(\zeta\omega T)\sin\left(\omega\sqrt{1-\zeta^2}T\right) = 2A\omega\sqrt{1-\zeta^2}(-\zeta\,\omega+\phi\,\psi) \tag{35}$$

Solving Eqs. (34) and (35) results in

$$\tan\left(\omega\sqrt{1-\zeta^2}T\right) = 2\,\frac{\omega\sqrt{1-\zeta^2}(-\zeta\,\omega+\phi\,\psi)}{-2\,\omega^2\zeta^2+\omega^2+2\,\phi\,\psi\,\zeta\,\omega-\psi^2} \tag{36}$$

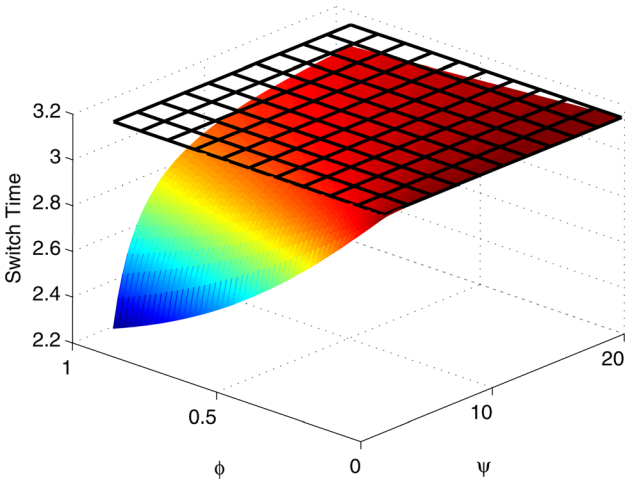

Fig. 9 Variation of switch time versus $\phi-\psi$

which leads to the switch time T

$$T = \pm\frac{n\pi}{\omega\sqrt{1-\zeta^2}} + \frac{1}{\omega\sqrt{1-\zeta^2}} \times \arctan\left(\frac{2\omega\sqrt{1-\zeta^2}(-\zeta\,\omega+\phi\,\psi)}{-2\,\omega^2\zeta^2+\omega^2+2\,\phi\,\psi\,\zeta\,\omega-\psi^2}\right) \tag{37}$$

which can be used to solve for A

$$A^2 = \frac{e^{2T\zeta\omega}}{4\,\omega^2\zeta^2\psi^2+\omega^4-4\,\omega^3\phi\,\psi\,\zeta-2\,\omega^2\psi^2-4\,\phi\,\psi^3\zeta\,\omega+\psi^4+4\,\omega^2\phi^2\psi^2} \tag{38}$$

Figure 9 illustrates the variation of the switch time, which is also the maneuver time as a function of the ϕ and ψ, which define the complex zeros of the transfer function. The second order poles of the system in consideration are characterized by a natural frequency of unity and a damping ratio of zero. ϕ which corresponds to the damping ratio of the zeros ranges from 0 to 1 and ψ which corresponds to the natural frequency range from 2 to 10. The mesh plane in Fig. 9 corresponds to the switch time of the standard input shaper. It can be seen that the pole-zero canceling input shaper always outperforms the standard input shaper. Likewise, Fig. 10 illustrates the variation of the gain of the postactuation filter as a function of ϕ and ψ, which is both below and above 0.5, which corresponds to the gain of the standard input shaper.

3.1 Example. To illustrate the proposed design, consider the example,

$$G_p(s) = \frac{s^2+2s+3}{s^2+2} \tag{39}$$

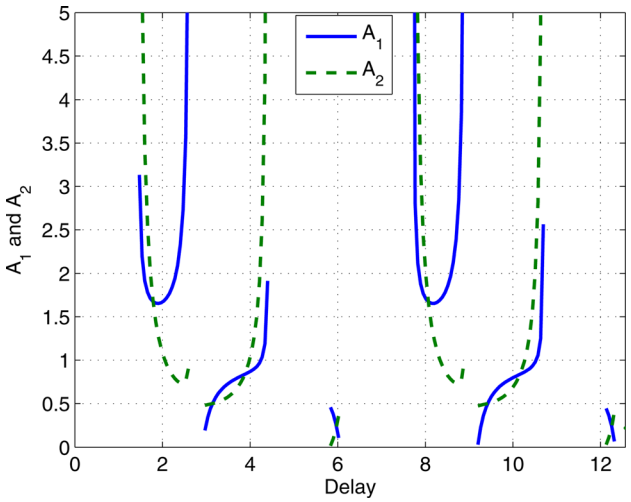

Fig. 8 Variation of positive normalized gains versus *T*

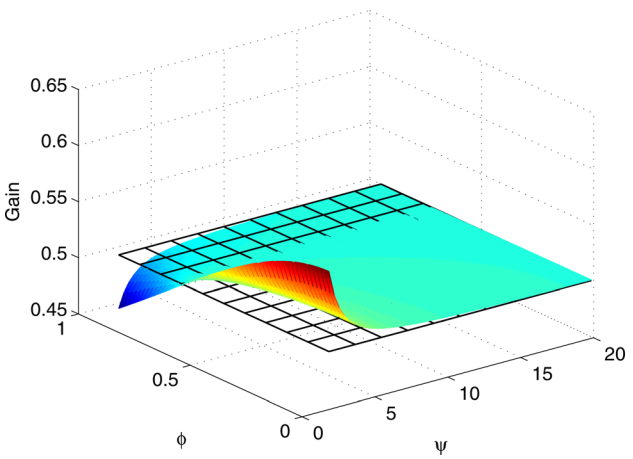

Fig. 10 Variation of gains versus $\phi-\psi$

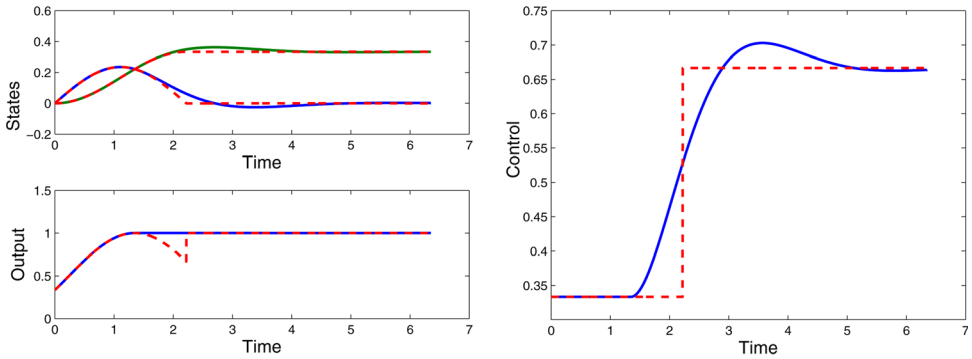

(a) Evolution of states (b) Control Profile

Fig. 11 Postactuated time-delay filter: (*a*) evolution of states; (*b*) control profile

we note that the dc gain is 1.5, which requires the final value of the output of the prefilter be scaled by $\frac{2}{3}$ to track a desired reference input. The resulting solution is

$$G(s) = 0.3333 + 1.0000\frac{\exp(-1.3510s)}{s^2 + 2s + 3} \tag{40}$$

The solution of the traditional input shaper is

$$G(s) = \frac{2}{3} + \frac{2}{3}\exp(-2.22144s) \tag{41}$$

Figures 11(*a*) and 11(*b*) illustrate the response of the pole-zero canceling input shaper (solid line). The dashed line is the solution of the traditional input shaper and illustrates that the maneuver takes longer to complete. One can note the jump discontinuity in the evolution of the output at time = 2.22 in Fig. 11(*a*) when the system is subject to the traditional input shaper. This is due to the fact that the system has a nonzero direct feed through of the input to the output.

The previous development catered to a complex conjugate pair of zeros. For systems which are characterized by two real zeros, the transfer function can be represented as

$$G_p(s) = \frac{(s+\alpha)(s+\beta)}{s^2 + 2\zeta\omega s + \omega^2}, \quad \alpha > 0, \beta > 0 \tag{42}$$

We require a time-delay filter with a transfer function

$$G(s) = A + \frac{\exp(-sT)}{(s+\alpha)(s+\beta)} \tag{43}$$

to cancel the poles and zeros of the transfer function of the system to be controlled. Following the same procedure presented for the first and second order zeros, we can solve for the switch time and the pole-zero canceling input shaper gain as

$$\tan(\omega\sqrt{1-\zeta^2}T) = \frac{\omega\sqrt{1-\zeta^2}(2\zeta\omega - \beta - \alpha)}{2\omega^2\zeta^2 - \zeta\omega\beta - \omega^2 - \alpha\zeta\omega + \alpha\beta} \tag{44}$$

$$A^2 = \frac{e^{2T\zeta\omega}}{\alpha^2\beta^2 + \omega^2\beta^2 + \omega^2\alpha^2 + 4\omega^2\zeta^2\alpha\beta + \omega^4 - 2\zeta\omega\beta^2\alpha - 2\alpha^2\zeta\omega\beta - 2\zeta\omega^3\beta - 2\omega^3\alpha\zeta} \tag{45}$$

Figure 12 illustrates the variation of the switch time, which is also the maneuver time as a function of α and β, which correspond to two real zeros of the transfer function. The mesh plane in Fig. 12 corresponds to the switch time of the standard input shaper. Likewise Fig. 13 illustrates the variation of the gain of the postactuation filter as a function of α and β.

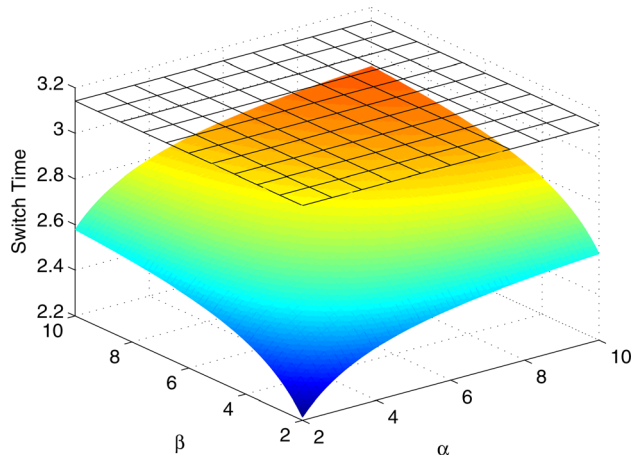

Fig. 12 Variation of switch time versus $\alpha - \beta$

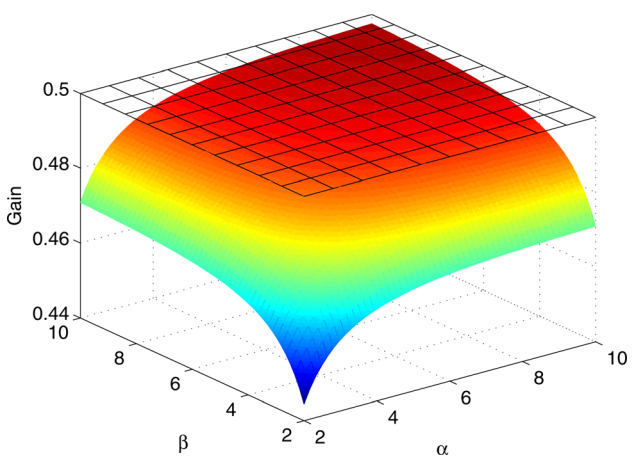

Fig. 13 Variation of gains versus $\alpha - \beta$

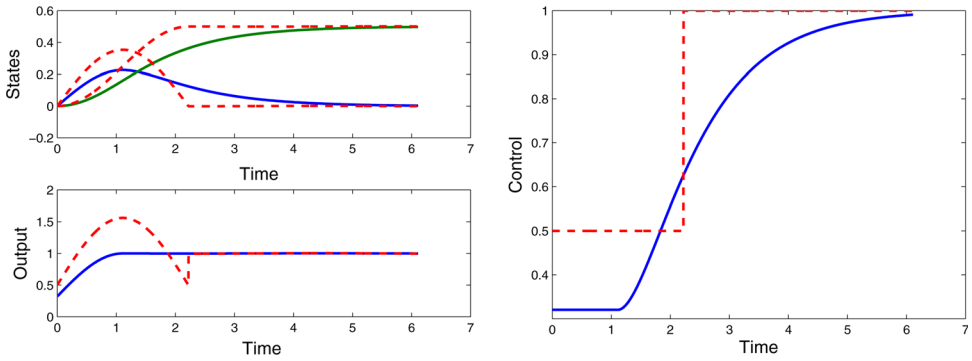

(a) Evolution of states (b) Control Profile

Fig. 14 Postactuated time-delay filter: (*a*) evolution of states; (*b*) control profile

3.2 Example. For the example,

$$G_p(s) = \frac{(s+1)(s+2)}{s^2+2} \tag{46}$$

we note that the dc gain is 1, which requires the final value of the output should equal to 1, to track a desired reference input. The resulting solution is

$$G(s) = 0.3204 + 1.3592\frac{\exp(-1.1107s)}{(s+1)(s+2)} \tag{47}$$

Figures 14(*a*) and 14(*b*) compare the performance of the proposed and traditional input shapers.

Having illustrated the technique to cancel the poles and zeros of the system with the zeros and poles of the transfer function of a time-delay filter for a second order system, we will generalize the proposed technique for a multipole and multizero system in Sec. 4.

4 Generalization

Consider a stable or marginally stable transfer function of the form

$$\frac{Y(s)}{U(s)} = G_p(s) = \frac{\sum_{i=0}^{m} a_i s^i}{s^n + \sum_{j=0}^{n-1} b_j s^j} \tag{48}$$

where $n \geq m$. All the zeros of the plant $G_p(s)$ are assumed to lie in the left-half of the complex plane. For systems which include non-minimum phase zeros, only the left-half plane zeros are considered in the design.

For the design of a postactuation time-delay filter, consider the parameterization

$$\frac{U(s)}{R(s)} = G_c(s) = A_{L+1}\frac{\exp(-sT_L)}{\sum_{i=0}^{m} a_i s^i} + \sum_{k=0}^{L} A_k \exp(-sT_k) \tag{49}$$

where $T_0 = 0$. The parameters of the time-delay filter, i.e., A_k and T_k need to satisfy the constraints

$$G_c(s = -p_j) = 0, \forall p_j = \text{roots}(s^n + \sum_{j=0}^{n-1} b_j s^j) \tag{50}$$

which guarantee cancelation of all the poles of the system with zeros of the time-delay filter. To ensure that the final values of the desired step input of magnitude y_f is achieved, we require

$$y_f = \lim_{s\to 0}\frac{1}{s} sG_cG_p = \frac{a_0}{b_0}\left(\frac{A_{L+1}}{a_0} + \sum_{k=0}^{L} A_k\right) \tag{51}$$

To reduce the sensitivity of the shaped input to errors in modeling uncertainties, which are reflected in the errors in the location of the poles of the system, we require

$$\frac{dG_c}{ds}(s = -p_u) = 0 \tag{52}$$

$$-A_{L+1}T_L\frac{\exp(-sT_L)}{\sum_{i=0}^{m} a_i s^i} - A_{L+1}\frac{\exp(-sT_L)\sum_{i=1}^{m} i a_i s^{i-1}}{\left(\sum_{i=0}^{m} a_i s^i\right)^2} - \sum_{k=1}^{L} A_k T_k \exp(-sT_k) = 0$$

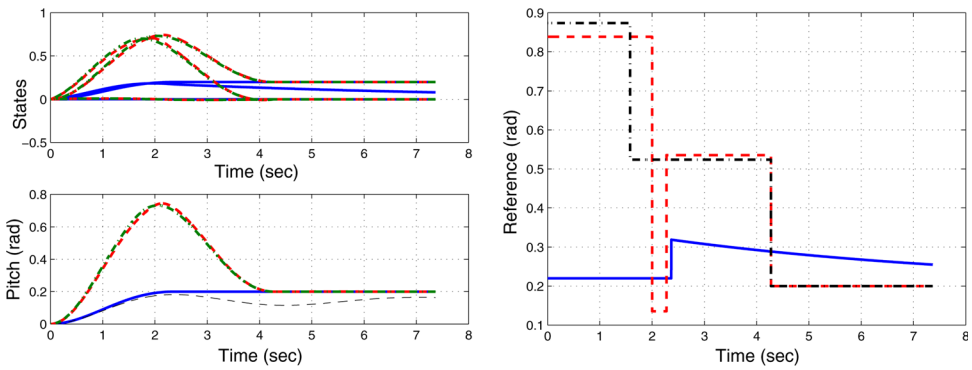

(a) Evolution of states (b) Control Profile

Fig. 15 Postactuated time-delay filter: (*a*) evolution of states; (*b*) control profile

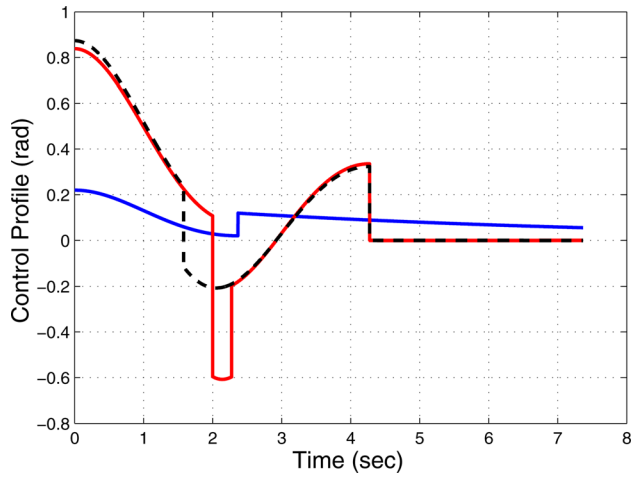

Fig. 16 Elevator deflection profile

where p_u is the uncertain pole. An optimization problem can be posed to determine the parameters of the postactuation time-delay filter. The statement of the problem is

$$\min J = T_L \tag{53a}$$

subject to

$$A_{L+1}\frac{\exp(-sT_L)}{\sum_{i=0}^{m} a_i s^i} + \sum_{k=0}^{L} A_k \exp(-sT_k)\Big|_{s=-p_j} = 0 \forall p_j \tag{53b}$$

$$-A_{L+1}\frac{\exp(-sT_L)}{\sum_{i=0}^{m} a_i s^i}\left(T_L + \frac{\sum_{i=1}^{m} i a_i s^{i-1}}{\sum_{i=0}^{m} a_i s^i}\right) - \sum_{k=1}^{L} A_k T_k \exp(-sT_k)\Big|_{s=-p_j} = 0 \tag{53c}$$

$$\frac{a_0}{b_0}\left(\frac{A_{L+1}}{a_0} + \sum_{k=0}^{L} A_k\right) = y_f \tag{53d}$$

$$T_L > T_{L-1} > \ldots > T_2 > T_1 > 0 \tag{53e}$$

5 Example

Consider the problem of pitch control of an aircraft. The transfer function relating the elevator deflection to the pitch motion is [18]

$$\frac{\theta(s)}{\delta_e(s)} = \frac{1.151s + 0.1774}{s^3 + 0.739s^2 + 0.921s} \tag{54}$$

Assume a proportional feedback controller with a gain of unity. The resulting closed-loop system dynamics are

$$\frac{\theta(s)}{R(s)} = \frac{1.151s + 0.1774}{s^3 + 0.739s^2 + 2.072s + 0.1774} \tag{55}$$

where $R(s)$ is the reference input to the system. The closed-loop poles and zeros are located at

$$\text{Poles} = \begin{bmatrix} -0.3255 + 1.3816i \\ -0.3255 - 1.3816i \\ -0.0881 \end{bmatrix} \quad \text{Zeros} = [-0.15413] \tag{56}$$

Parameterize the postactuating time-delay filter as

$$R_1(s) = \frac{0.2}{s}\left(A_1 + A_2\exp(-sT_1) + \frac{A_3}{s + 0.15413}\exp(-sT_1)\right) \tag{57}$$

Solving a parameter optimization problem so as to cancel all the poles and zeros of the closed-loop transfer function results in the time-delay filter

$$R_1(s) = \frac{1}{s}(0.2198 + 0.0993\exp(-2.3673s) + \frac{-0.0184}{s + 0.15412}\exp(-2.3673s)) \tag{58}$$

To compare the performance to the standard input shaper/time-delay filter, a time-delay filter is parameterized as

$$R_2(s) = \frac{0.2}{s}(A_1 + A_2\exp(-sT_1) + A_3\exp(-sT_2)) \tag{59}$$

The five unknown parameters need to satisfy four constraints. Arbitrarily bounding the time-delay gains A_i as

$$-0.35 \le A_i \le 2 \tag{60}$$

results in the time-delay filter

$$R_2(s) = \frac{1}{s}(0.8735 - 0.350\exp(-1.5783s) - 0.3235\exp(-4.2744s)) \tag{61}$$

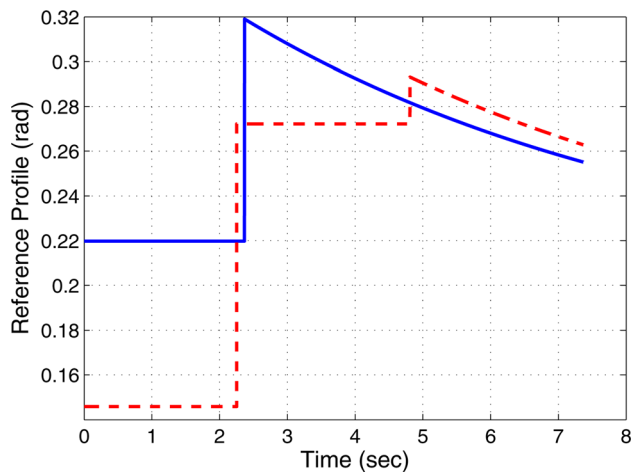

Fig. 17 Postactuation reference profiles

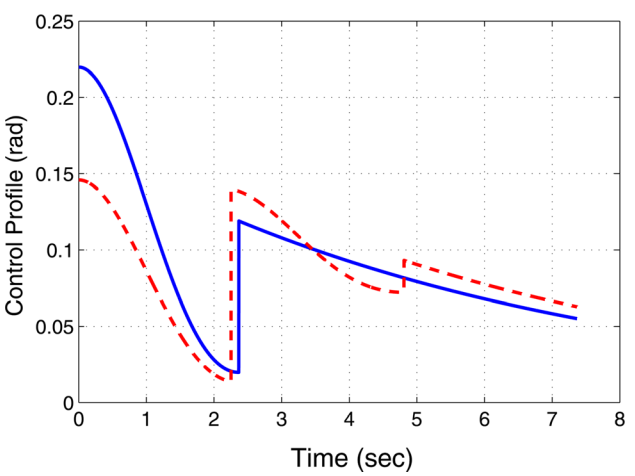

Fig. 18 Elevator deflection profiles

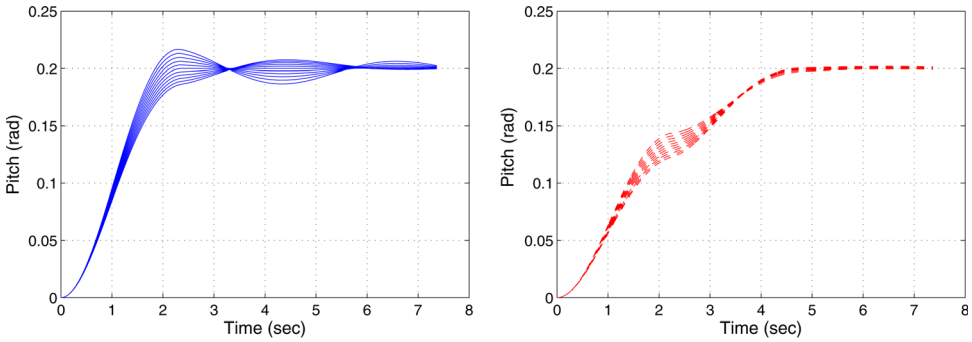

Fig. 19 Comparison of the nonrobust and robust postactuation filters: (*a*) output (nonrobust); (*b*) output (robust)

Finally, a time-delay filter designed by convolving time-delay filters designed sequentially to cancel the poles of the system with the constraint that the final time of the filter is the same as that of the concurrent time-delay filter design, i.e., $T_2 = 4.2744$. The time-delay filter is parameterized as

$$R_3(s) = \frac{0.2}{s}(A_1 + A_2\exp(-sT_1))(A_3 + A_4\exp(-sT_2)) \quad (62)$$

where the first filter is used to cancel the underdamped poles at $-0.3255 \pm 1.3816i$, which results in the filter

$$(A_1 + A_2\exp(-sT_1)) = 0.6770 + 0.3229\exp(-2.2739s) \quad (63)$$

The second filter's delay time is selected to be $T_2 = 4.2744 - 2.2739$. The gains A_3 and A_4 to cancel the pole at $s = -0.0881$ is given as

$$(A_3 + A_4\exp(-sT_2)) = 6.1916 - 5.1916\exp(-2.0004s) \quad (64)$$

Figure 15(*b*) illustrates the shaped reference profiles. The solid line corresponds to the postactuation filter, the dashed line to the cascaded input shaper and the dashed-dotted line to the concurrently designed input shaper. The time-delay of the input shaper to cancel the first order pole is selected to result in the same maneuver time as the concurrently designed input shaper. It is clear from Fig. 15(*b*) that the magnitude of the applied reference signal for the traditional input shapers are significantly greater than the postactuation input shaper. The same can be gauged from Fig. 16, which illustrates the evolution of the control input to the system. The benefit of the postactuation filter is evident from the small domain over which the control input varies as compared to the traditional input shaper. Finally, the maneuver time of the postactuation filter is about 45% smaller than the traditional input shapers.

To illustrate the benefit of desensitizing the postactuation reference profile, assume that the coefficient of the s^2 term in the denominator of the transfer function is uncertain and can lie in a $\pm 30\%$ off its nominal values. This would result in uncertainties in the location of the closed-loop poles. Locating multiple zeros of the postactuation filter at the estimated location of the poles of the system results in a postactuation filter whose transfer function is

$$R_4(s) = \frac{1}{s}(0.1458 + 0.1263\exp(-2.2521s) + 0.0210\exp(-4.8108s) + \frac{-0.0144}{s + 0.15412}\exp(-4.8108s)) \quad (65)$$

Figure 17 compares the shaped reference profiles for the nonrobust (dashed line) and the robust (solid line) cases. It is clear from the transfer functions $R_1(s)$ and $R_4(s)$ that the improving the sensitivity to model uncertainties is achieved by an increase in the maneuver time. Figure 18 illustrates the actuator motions for the two cases and the robust case (solid line) demands a smaller range of motion of the elevator.

To illustrate the robustness of the desensitized command profile, 11 simulations were carried out for systems where the uncertain parameter spanned the entire uncertain region uniformly. Figures 19(*a*) and 19(*b*) clearly illustrate that the excursion of the system response is much smaller for the robust command profile compared to the nonrobust command profile.

6 Conclusions

Traditional input shapers/time-delay filters are designed so as to cancel the poles of the system with the intent of eliminating residual motion at the end of the maneuver. This paper augments the pole cancelation approach with a simple technique to cancel the zeros of the transfer function of the system with poles of the time-delay prefilter. The consequence of this pole-zero cancelation and the zero-pole cancelation is a reduction in the maneuver time for the output of interest. The output of the system is at steady state despite the control and states of the system continuing to transition to their final values.

Robustness to uncertainties in system poles are addressed by locating multiple zeros of the time-delay filter at the estimated location of the uncertain poles. The proposed technique is illustrated on simple examples and on the pitch control of an aircraft.

References

[1] Tallman, G. H., and Smith, O. J. M., 1958, "Analog Study of Posicast Control," IRE Trans. Autom. Control, **3**, pp. 14–21.
[2] Singer, N. C., and Seering, W. P., 1990, "Preshaping Command Inputs to Reduce System Vibrations," ASME J. Dyn. Syst., Meas., Control, **112**, pp. 76–82.
[3] Singh, T., and Vadali, S. R., 1993, "Robust Time-Delay Control," ASME J. Dyn. Syst., Meas., Control, **115**, pp. 303–306.
[4] Bhat, S. P., and Miu, D. K., 1990, "Precise Point-to-Point Positioning Control of Flexible Structures," ASME J. Dyn. Syst., Meas., Control, **112**(4), pp. 667–674.
[5] http://www.wdc.com/en/
[6] Hindle, T., and Singh, T., 2001, "Robust Minimum Power/Jerk Control of Maneuvering Structures," AIAA J. Guid. Control Dyn., **24**(4), pp. 816–826.
[7] Singh, T., 2004, "Jerk Limited Input Shapers," ASME J. Dyn. Syst., Meas., Control, **126**(1), pp. 215–219.
[8] Sorensen, K. L., Singhose, W., and Dickerson, S 2008, "A Controller Enabling Precise Positioning and Sway Reduction in bridge and Gantry Cranes," Control Eng. Pract., **15**, pp. 825–837.
[9] Schitter, G., Thurner, P. J., and Hansma, P. K., 2008, "Design and Input-Shaping Control of a Novel Scanner for High-Speed Atomic Force Microscopy," Mechatronics, **18**, pp. 282–288.
[10] Singhose, W., Singer, N., and Seering, W., 1996, "Improving Repeatability of Coordinate Measuring Machines With Shaped Command Signals," Precis. Eng., **18**, pp. 138–146.
[11] Seth, N., Rattan, K., and Brandstetter, R., 1993, "Vibration Control of a Coordinate Measuring Machine," IEEE Conference on Control Applications, Dayton, OH.

[12] Jones, S., and Ulsoy, A. G., 1999, "An Approach to Control Input Shaping With Application to Coordinate Measuring Machines," ASME J. Dyn. Syst., Meas., Control, **121**, pp. 242–247.
[13] Smith, O. J. M., 1957, "Posicast Control of Damped Oscillatory Systems," Proc. IRE, **1**, pp. 1249–1255.
[14] Singhose, W., Derezinski, S., and Singer, N., 1996, "Extra-Insensitive Input Shapers for Controlling Flexible Spacecraft," AIAA J. Guid. Control Dyn., **19**, pp. 385–391.
[15] Singh, T., 2002, "Minimax Design of Robust Controllers for Flexible Systems," AIAA J. Guid. Control Dyn., **25**(5), pp. 868–875.
[16] Perez, H., and Devasia, S., 2003, "Optimal Output-Transition for Linear Systems," Automatica, **39**, pp. 181–192.
[17] Iamratanakul, D., Jordan, B., Leang, K., and Devasia, S., 2008, "Optimal Output Transitions for Dual-Stage Systems," IEEE Trans. Control Syst. Technol., **16**(5), pp. 869–991.
[18] http://www.engin.umich.edu/class/ctms/